Local Structure of Isolated Positively Charged Muonium as an Analog for the Hydrogen Ion in *p*-Type GaAs

B. E. Schultz,[1] K. H. Chow,[1] B. Hitti,[2] R. F. Kiefl,[2,3] R. L. Lichti,[4] and S. F. J. Cox[5,6]

[1]*Department of Physics, University of Alberta, Edmonton, Canada T6G 2J1*
[2]*TRIUMF, 4004 Wesbrook Mall, Vancouver, Canada V6T 2A3*
[3]*Canadian Institute for Advanced Research, University of British Columbia, Vancouver, Canada V6T 1Z1*
[4]*Department of Physics, Texas Tech University, Lubbock, Texas 79409-1051, USA*
[5]*ISIS Facility, Rutherford Appleton Laboratory, Chilton OX11 0QX, United Kingdom*
[6]*Department of Physics and Astronomy, University College London, London WC1E 6BT, United Kingdom*

(Received 15 May 2005; published 18 August 2005)

We determine the local structure of isolated positively charged muonium (Mu^+) in heavily doped *p*-type GaAs based on muon level crossing resonance and zero applied field muon spin depolarization data. These measurements provide the first direct experimental confirmation that Mu^+, and by analogy H^+, is located within a stretched Ga-As bond. The distances between Mu^+ and the nearest neighbor Ga and As atoms are estimated to be 1.83 ± 0.10 Å and 1.76 ± 0.10 Å, respectively. These results are compared to existing theoretical calculations on the structure of hydrogen in GaAs and additionally provide data on the induced electric field gradients.

DOI: 10.1103/PhysRevLett.95.086404 PACS numbers: 71.55.Eq, 76.60.Gv, 76.75.+i

Hydrogen (H) is an important interstitial impurity that easily enters into many elemental and compound semiconductors. Once inside the material, it can modify the optical and electronic properties of the host by reacting with deliberate dopants and other defects or by itself acting as a dopant. This has led to considerable experimental and theoretical work aimed at obtaining an accurate atomic-level description of hydrogen-related complexes and the precursor *isolated* hydrogen impurities [1]. Nevertheless, direct experimental identification and structural characterization of the three charge states of isolated atomic hydrogen, i.e., H^+, H^0, and H^-, is sparse. The charged centers are particularly difficult to characterize since they lack a magnetic hyperfine interaction, from which structural detail is obtained in standard magnetic resonance methods such as EPR and electron-nuclear double resonance. Thus far, of the charged isolated hydrogen centers, only H^+ in Si and both H^+ and H^- in Ge have been identified [2–5], via infrared absorption spectroscopy in each case.

No analogous experimental reports exist for H^+ or H^- in III-V semiconductors. Theory predicts that the charge state of isolated H depends on the Fermi level [6]. In particular, H^+ is the stable state in heavily doped *p*-type GaAs while H^- is formed in heavily doped *n*-type samples. Furthermore, H^+ and H^- are expected to be stable at very different sites in GaAs [6,7]: H^+ near the bond-center (BC) position and H^- at the tetrahedral site surrounded by Ga atoms (T_{Ga}), or antibonding (AB) to Ga slightly displaced from that location.

When isolated H cannot be studied directly, information on the charged states of H can be indirectly obtained by investigating its muonium ($Mu^0 = \mu^+ e^-$) counterpart [8–10]. If zero-point effects due to the lighter mass of the muon are unimportant, the ground state structures of H and Mu centers should be nearly the same. Considerable information has been obtained on the structure of (paramagnetic) Mu^0 centers [11,12] in several semiconductors through studies of the muon and nuclear hyperfine interactions. By contrast, the (diamagnetic) Mu^+ and Mu^- states are more difficult to characterize. In heavily doped GaAs, only diamagnetic muonium centers are observed. Although their charge has not been directly determined [13], the stability, kinetics, and structure of the diamagnetic Mu states in *n*-type [14,15] and *p*-type [16] GaAs are dramatically different, establishing that they are, indeed, distinct centers. Consistency with theory leads to the assignment of Mu^- in *n*-type and Mu^+ in *p*-type GaAs.

While the BC site for H^+ impurities in cubic semiconductors is now well accepted based on the theoretical results, no experimental evidence yet exists that conclusively demonstrates the BC structure for positively charged isolated hydrogen, i.e., an interstitial proton. In this Letter we present results that experimentally define the local structure of isolated Mu^+, and by analogy isolated H^+, in heavily doped *p*-type GaAs. In GaAs, all the host nuclei have a nuclear spin of 3/2 (^{69}Ga, 60.1% abundant; ^{71}Ga, 39.9% abundant; ^{75}As, 100% abundant). By using the muon level crossing resonance (μLCR) and zero-field techniques to study the dipolar and quadrupolar interactions associated with the muon and host atoms, we establish that isolated Mu^+ is, indeed, located within a Ga-As bond. The distances between the muon and nearest neighbor Ga and As atoms are estimated to be 1.83 ± 0.10 Å and 1.76 ± 0.10 Å, respectively, implying that the Ga-As bond is stretched by $\approx 47\%$. This work represents the most direct confirmation of the predicted BC site and first detailed structural characterization for isolated positively charged hydrogen or muonium in any semiconductor.

The structure we find for Mu^+ is compared with calculations on isolated H^+. Isolated Mu^- in GaAs is the only other charged muonium center in a semiconductor whose local structure has previously been characterized in similar detail [14].

The experiments [10] were carried out on the M15 and M20B channels at TRIUMF where nearly 100% polarized muons with a nominal momentum of $\approx$30 MeV/c are implanted into the sample. One $\langle 111\rangle$ and two $\langle 100\rangle$-oriented heavily doped p-type GaAs:Zn samples were studied. The $\langle 100\rangle$ sample ($[\mathrm{Zn}] = 1.8$–4.4×10^{19} cm^{-3}) was obtained from Crystal Systems International, while the other ($[\mathrm{Zn}] = 2.8 \times 10^{19}$ cm^{-3}) was obtained from Laser Diode. The $\langle 111\rangle$ sample ($[\mathrm{Zn}] = 4 \times 10^{18}$ cm^{-3}) was from Atomergic. All data were taken at 50 K where Mu^+ is static [16]. In the μLCR experiments, a small square-wave modulated magnetic field ($\Delta^{\pm} \approx \pm 20$ G) was superimposed as the main field was stepped across the relevant range. The difference in asymmetry of positron rates for the two modulation settings were recorded to reduce the effect of slow beam fluctuations. The μLCR signal, as seen in the accompanying figures, thus mimics a derivative. In the zero-field measurements, the field was zeroed to ≈ 1 μT.

The data are modeled using a spin Hamiltonian $\mathcal{H}$ that describes Mu^+ interacting with neighboring Ga and As nuclei; interactions between host nuclei are extremely small and are ignored. The Hamiltonian thus consists of terms for the muon and nuclear Zeeman interactions, the magnetic dipole coupling between the muon and nucleus **D**, and the nuclear electric quadrupole interaction **Q** arising from a muon-induced electric field gradient at the nucleus. Hence,

$$\begin{aligned}\mathcal{H} = & -\tilde{\gamma}_\mu B I_z - \tilde{\gamma}_{\mathrm{Ga}} B J_z - \tilde{\gamma}_{\mathrm{As}} B K_z \\ & + D^{\mathrm{Ga}}(-2I_{z'}J_{z'} + I_{x'}J_{x'} + I_{y'}J_{y'}) \\ & + D^{\mathrm{As}}(-2I_{z'}K_{z'} + I_{x'}K_{x'} + I_{y'}K_{y'}) \\ & + Q^{\mathrm{Ga}}\left(J_{z'}^2 - \frac{J(J+1)}{3}\right) + Q^{\mathrm{As}}\left(K_{z'}^2 - \frac{K(K+1)}{3}\right), \quad (1)\end{aligned}$$

where **I**, **J**, and **K** are the muon, gallium, and arsenic spin operators, respectively (for Ga and As, $J = K = 3/2$). The magnetic field **B** is applied parallel to the initial muon spin for μLCR measurements and defines the z axis. The dipolar and nuclear electric quadrupole tensors are assumed to be axially symmetric around the muon-nucleus direction z' which is at an angle θ with respect to z. The dipole and quadrupole parameters are

$$D^i = \frac{\mu_0 h \tilde{\gamma}_\mu \tilde{\gamma}_i}{4\pi r_i^3}, \qquad Q^i = \frac{V_{z'z'}^i \mathrm{eq}^i}{4}, \qquad (2)$$

where r_i is the muon-nucleus separation, μ_0 is the permeability of free space, h is Planck's constant, $\tilde{\gamma}_\mu$ is the gyromagnetic ratio of the muon (135.5374 MHz/T), $\tilde{\gamma}_i$ is the gyromagnetic ratio of nucleus i (known for ^{69}Ga, ^{71}Ga, and ^{75}As), eq^i is the electric quadrupole moment of nucleus i, and $V_{z'z'}^i$ is the electric field gradient at nucleus i. The eigenvalues and eigenvectors of the spin Hamiltonian are numerically calculated and used to simulate the time-integrated polarization $\bar{P}_z$ along **B**, which is the quantity of interest in a μLCR experiment, or to model the time evolution of $P_z(t)$ [10,17].

The simulations shown in Fig. 1 for a system consisting of a muon and one spin 3/2 nucleus illustrate the principles behind a μLCR experiment. (Although we have used the full Hamiltonian in our analysis, the μLCRs are very well approximated by considering interactions with a *single* nucleus since experimentally they turn out to be located at very different magnetic fields [9,10,17]). At most magnetic fields, the Zeeman splitting for the muon is very different from the combined Zeeman and quadrupole splittings for the neighboring nucleus, and the muon spin remains aligned along **B** with $\bar{P}_z = 1$. At a μLCR, however, the energy splittings for the muon and nucleus are equal [Fig. 1(a)] and the dipolar coupling leads to a resonant transfer of polarization from the muon to the nucleus; hence, $\bar{P}_z$ is reduced at these magnetic fields and appears as a "resonance" [Fig. 1(b)]. In a μLCR experiment, one varies the magnetic field and searches for these resonances, which are then used to characterize the local structure of Mu^+; that is, they are used to identify the nearest neighbor

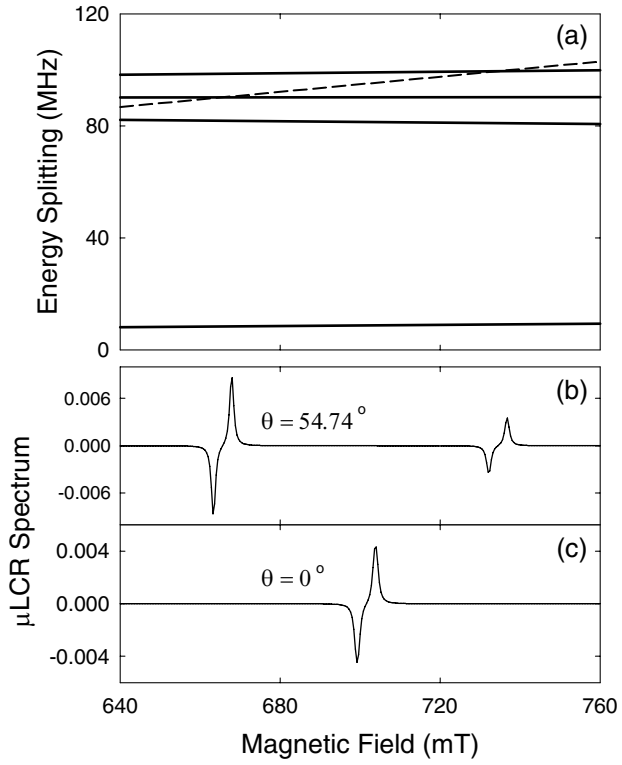

FIG. 1. (a) Magnetic field dependence of energy splittings for a muon (dashed line) and a spin 3/2 As nucleus (solid lines) with $\tilde{\gamma}_{\mathrm{As}} = 7.292$ MHz, $Q^{\mathrm{As}} = 44.970$ MHz, and $\theta = 54.74°$; (b) the corresponding As μLCR spectra; and (c) the single resonance for $\theta = 0°$.

atom(s) and obtain the muon-nucleus separation distance and direction.

The position of a resonance for a particular angle θ depends linearly on the quadrupole interaction Q which is proportional to the quadrupole moment of the nucleus [Eq. (2)]. The existence (or lack) of an isotopic partner allows each resonance to be specifically attributed to a ^{69}Ga, ^{71}Ga, or ^{75}As neighbor. Once the nucleus is identified and Q obtained, two methods are available to determine the muon-to-nucleus direction, i.e., θ: (a) a small companion resonance is present for certain values of θ [Fig. 1(b)] whose position at higher fields relative to the main line is strongly dependent on θ, or (b) the position of the main resonance itself depends on θ [cf Figs. 1(b) and 1(c)]. Finally, for a given Q and θ, the amplitude of the resonance depends on the muon-nuclear dipolar coupling D, which in turn depends on the muon-nucleus separation distance [Eq. (2)].

An initial search for μLCR resonances was carried out with **B** parallel to a $\langle 100 \rangle$ crystal direction. A total of three ''main'' resonances were located, two of which are shown in Fig. 2(a) (192.0 mT) and Fig. 2(b) (665.6 mT). The third resonance, at $B = 304.0$ mT, is not displayed. The resonance in Fig. 2(a) is unambiguously assigned to ^{71}Ga and the one at 304.0 mT to ^{69}Ga by the excellent agreement between the ratio of resonant fields (1.583) compared to the ratio of the quadrupole moments for the two Ga isotopes ($q^{69}/q^{71} = 0.178/0.112 = 1.589$). Similarly, the resonance in Fig. 2(b) is assigned to ^{75}As (isotope abundance 100%) since it has no Ga isotopic companion. Similar sized resonances due to Ga and As imply that both nuclei are close neighbors to the muon.

Having identified the near neighbors, the symmetry of the muon site is obtained from the resonant fields for **B** along $\langle 110 \rangle$ and $\langle 111 \rangle$ compared to those for $\langle 100 \rangle$. As illustrated in Figs. 2(c) and 2(d) for **B** $\parallel \langle 111 \rangle$, the ^{71}Ga and ^{75}As resonances are shifted significantly. By comparing the data in Fig. 2 with the simulations using Eq. (1), we determined that both the Ga and As neighbors lie along $\langle 111 \rangle$, i.e., a bond direction. Specifically, within the accuracy of the applied field alignment, the μLCR resonances in Figs. 2(a) and 2(b) correspond to $\theta = 54.74°$ and the spectra in Figs. 2(c) and 2(d) contain contributions from $\theta = 0°$ and $\theta = 70.53°$. A further consistency check is shown for the ^{75}As spectrum [Fig. 2(b)] with **B** $\parallel \langle 100 \rangle$: the position of the small satellite resonance is well reproduced. Additionally, a single value of $Q^{71} = 12.8875 \pm 0.0015$ MHz and $Q^{75} = 49.970 \pm 0.004$ MHz reproduces the positions of all the observed μLCR data for Ga and As, respectively. At this stage, either the BC or the AB sites would, in principle, be consistent with the observed symmetry of the Ga and As near-neighbor directions.

An estimate of the distance between the muon and the neighboring Ga and As nuclei can be obtained from the μLCR amplitudes since they depend on the dipolar interaction. A good orientation for carrying out this exercise is **B** $\parallel \langle 111 \rangle$, where the strongest resonance is due to a single bond at 0° and is hence insensitive to slight misorientations of the crystal with respect to the field, while the rest of the spectrum is due to the three bonds at 70.53°. By contrast, for **B** $\parallel \langle 100 \rangle$, all four bonds are at 54.74° and a small misalignment broadens the resonance, making it difficult to ascertain the correct amplitude. Fits to the ^{71}Ga and ^{75}As resonances for **B** $\parallel \langle 111 \rangle$ [Figs. 2(c) and 2(d)] yield values of $D^{71} = 0.019 \pm 0.003$ MHz and $D^{75} = 0.012 \pm 0.002$ MHz. Using Eq. (2), we estimate the Mu^+-Ga and Mu^+-As distances to be $r_{Ga} = 1.83 \pm 0.10$ Å and $r_{As} = 1.76 \pm 0.10$ Å. The similarity between r_{Ga} and r_{As} rules out the AB location, and strongly implies that the muon is located in a BC site with the bond stretched by $\approx 47\%$ compared to its undistorted length (2.45 Å). The same D values, combined with the Q values obtained above, produce the solid lines in Figs. 2(a) and 2(b) where **B** $\parallel \langle 100 \rangle$. The discrepancy between the simulations and the data is attributed to a small misorientation of the crystal as discussed above.

Finally, in order to confirm that the observed μLCRs are, indeed, due to the two nearest neighbors to the muon, i.e., that there are no other resonances that are located at magnetic fields beyond the search region, we measured $P_z(t)$ in the absence of an applied magnetic field (see Fig. 3). Here, the muon polarization evolves under the influence of the dipole interaction; qualitatively, the larger the dipolar interaction, the faster the polarization relaxes. The shaded area represents the possible range for $P_z(t)$ based on Eq. (1) and the experimental range of D^i's and

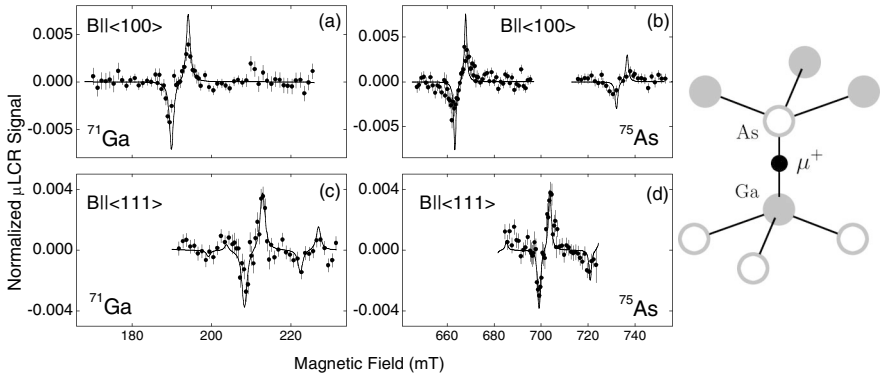

FIG. 2. Experimental data for ^{71}Ga with (a) B $\parallel \langle 100 \rangle$ ($\theta = 54.74°$) and (c) B $\parallel \langle 111 \rangle$ ($\theta = 0°$ and 70.53°), and for ^{75}As with (b) B $\parallel \langle 100 \rangle$ ($\theta = 54.74°$) and (d) B $\parallel \langle 111 \rangle$ ($\theta = 0°$ and 70.53°). Solid lines are simulations using best fit parameters as described in text. The attached picture is a diagram of the nearest neighbor nuclei, showing μ^+ at the BC position.

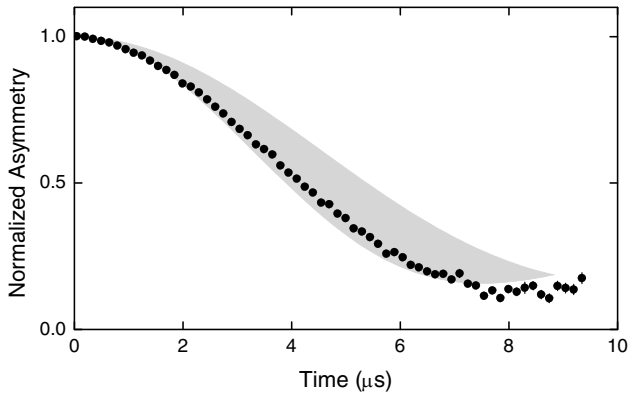

FIG. 3. Time dependence of zero-field muon polarization for $\theta = 54.74°$. Shaded area represents the uncertainty in the D^i values (see text).

Q^i's. The agreement between this calculation and the experiment is very good, verifying that the observed μLCR resonances are, indeed, the primary ones. The influence of second and further neighbors will slightly increase the depolarization rate from $P_z(t)$ as calculated from only the nearest Ga and As moments; thus the agreement is actually better than indicated.

Our current experimental results can be compared with theoretical calculations of the stable site for H^+. Pavesi *et al.* [6] and Breuer *et al.* [7] each predict that H^+ is located in a near bond-center position with H^+-Ga distances of 1.80 and 2.14 Å and H^+-As distances of 1.52 and 1.50 Å, respectively, yielding bond-stretch predictions of 36% and 49%.

In agreement with theory, our data imply that isolated Mu^+ is situated at a BC site with a significant outward distortion of the nearest neighbor Ga and As nuclei. However, we find that the muon is located much closer to the geometrical bond center than expected from predictions for H^+ in GaAs, which place the proton significantly closer to As than to Ga. It may be worth noting that experimental results [11] for Mu^0 in the BC site place the muon much closer to Ga than to As, while these same theoretical treatments find a much more symmetric location, and a third calculation [18] places H^+ slightly closer to As than to Ga. The differences may be a consequence of the large zero-point energy associated with the muon and an anharmonic potential energy surface. Further theoretical work would be useful in shedding some light on these discrepancies.

In summary, we have experimentally determined the structure of isolated Mu^+ in *p*-type GaAs. As expected from calculations on H^+ in GaAs, Mu^+ is located within a Ga-As bond. However, the average position of the muon is much closer to the geometrical center of the bond than predicted by theory for a classical (heavier) particle; effects of zero-point energy have not been predicted for either a muon or a proton. Our data additionally provide accurate values of local quadrupole interactions, providing a stringent test for more detailed structural calculations.

The research in this Letter and TRIUMF are partially supported by the National Sciences and Engineering Research Council of Canada. R. L. L. is supported by the U.S. National Science Foundation (DMR-102862) and Robert A. Welch Foundation (D-1321). We acknowledge A. N. MacDonald for assistance.

[1] S. J. Pearton, J. W. Corbett, and M. Stavola, *Hydrogen in Crystalline Semiconductors* (Springer, Berlin, 1992).
[2] H. J. Stein, Phys. Rev. Lett. **43**, 1030 (1979).
[3] M. Budde, Ph.D. thesis, Aarhus University, Denmark, 1998.
[4] M. Budde, G. Lüpke, C. Parks Cheney, N. H. Tolk, and L. C. Feldman, Phys. Rev. Lett. **85**, 1452 (2000).
[5] M. Budde, B. Bech Nielson, C. Parks Cheney, N. H. Tolk, and L. C. Feldman, Phys. Rev. Lett. **85**, 2965 (2000).
[6] L. Pavesi and P. Giannozzi, Phys. Rev. B **46**, 4621 (1992).
[7] S. J. Breuer, R. Jones, P. R. Briddon, and S. Öberg, Phys. Rev. B **53**, 16 289 (1996).
[8] B. D. Patterson, Rev. Mod. Phys. **60**, 69 (1988).
[9] R. F. Kiefl and T. L. Estle, in *Hydrogen in Semiconductors*, edited by J. Pankove and N. M. Johnson, Semiconductors and Semimetals Vol. 34 (Academic, New York, 1990), p. 547.
[10] K. H. Chow, B. Hitti, and R. F. Kiefl, in *Identification of Defects in Semiconductors*, edited by M. Stavola, Semiconductors and Semimetals Vol. 51A (Academic Press, New York, 1998), p. 137.
[11] R. F. Kiefl, M. Celio, T. L. Estle, G. M. Luke, S. R. Kreitzman, J. H. Brewer, D. R. Noakes, E. J. Ansaldo, and K. Nishiyama, Phys. Rev. Lett. **58**, 1780 (1987).
[12] J. W. Schneider, K. Chow, R. F. Kiefl, S. R. Kreitzman, A. MacFarlane, R. C. DuVarney, T. L. Estle, R. L. Lichti, and C. Schwab, Phys. Rev. B **47**, 10 193 (1993).
[13] K. L. Hoffman, K. H. Chow, R. F. Kiefl, B. Hitti, T. L. Estle, and R. L. Lichti, Physica (Amsterdam) **326B**, 175 (2003).
[14] K. H. Chow, R. F. Kiefl, W. A. MacFarlane, J. W. Schneider, D. W. Cooke, M. Leon, M. Paciotti, T. L. Estle, B. Hitti, R. L. Lichti, S. F. J. Cox, C. Schwab, E. A. Davis, A. Morrobel-Sosa, and L. Zavieh, Phys. Rev. B **51**, 14 762 (1995).
[15] K. H. Chow, B. Hitti, R. F. Kiefl, S. R. Dunsiger, R. L. Lichti, and T. L. Estle, Phys. Rev. Lett. **76**, 3790 (1996).
[16] K. H. Chow, B. Hitti, R. F. Kiefl, R. L. Lichti, and T. L. Estle, Phys. Rev. Lett. **87**, 216403 (2001); K. H. Chow, R. F. Kiefl, J. W. Schneider, T. L. Estle, B. Hitti, T. M. S. Johnson, R. L. Lichti, and W. A. MacFarlane, Hyperfine Interact. **86**, 645 (1994).
[17] R. F. Kiefl and S. R. Kreitzman in *Perspectives of Meson Science*, edited by T. Yamazaki *et al.* (Elsevier Science Publishers, Amsterdam, 1992), p. 265.
[18] Dj. M. Maric, S. Vogel, P. F. Meier, and S. K. Estreicher, Phys. Rev. B **40**, 8545 (1989).